

# The Generalized Gutzwiller Method for $n \geq 2$ Correlated Bands: First Order Metal-Insulator Transitions

J. Bünemann and W. Weber

*Institut für Physik, Universität Dortmund,*

*D-44221 Dortmund, Germany*

(October 6, 2018)

## Abstract

We have generalized the Gutzwiller method to the cases of  $n \geq 2$  correlated bands and report studies on a degenerate two-band model with Hund's rule type on-site interactions. At half band filling the metal-insulator transitions are usually of first order.

71.27.+a, 71.30.+h, 75.10.-b

## I. INTRODUCTION

The Gutzwiller variational method has been used since long for the study of ground state properties of Hubbard-type models for correlated fermions.<sup>1</sup> The one-band (one orbital) formulation has been extended in various ways to treat, e.g. antiferromagnetism<sup>2,3</sup> or to include additional, uncorrelated orbitals.<sup>4-6</sup> The Gutzwiller ansatz has also been investigated analytically.<sup>7</sup> However, attempts to extend the method to  $n = 2$  correlated orbitals per site have, so far, led to unsatisfactory results.<sup>8</sup>

In this paper we generalize the Gutzwiller method to cases of arbitrary numbers  $n$  of correlated orbitals per site. The extension makes it possible to study the ground state properties of realistic models for magnetic 3d transition metals and compounds. As a first application, we examine a two-band model with more general on-site interactions and focus on the metal-insulator transition<sup>9</sup> at quarter and half band fillings.

## II. GENERALIZATION OF THE GUTZWILLER METHOD

For one band, the Gutzwiller variational wavefunction reads as

$$|\Psi\rangle \equiv g^{\widehat{D}} |\Psi_0\rangle = \prod_{s=1}^L [1 - (1-g)\widehat{D}_s] |\Psi_0\rangle, \quad (1)$$

where  $|\Psi_0\rangle$  is an uncorrelated wavefunction on a lattice of  $L$  sites and the operators  $\widehat{D}_s \equiv \widehat{n}_{s\uparrow}\widehat{n}_{s\downarrow}$  measure the double occupancy of sites  $s$ . The variational parameter  $g$  will reduce the total number  $D \equiv \overline{M}_{12}$  of doubly occupied sites and may vary between  $g = 1$  ( $\overline{M}_{12} = M_1 M_2 / L$ ) and  $g = 0$  ( $\overline{M}_{12} = 0$ ). Here  $M_1$  ( $M_2$ ) are the gross numbers of spin up (down) sites. The norm of (1) is approximated by<sup>10</sup>

$$\langle \Psi | \Psi \rangle = P_1 P_2 \sum_D g^{2D} N_D(L, M_1, M_2), \quad (2)$$

with the probabilities  $P_k = M_k!(L - M_k)!/L!$  and the combinatorial weight factors

$$N_D \equiv \frac{L!}{\overline{M}_0! \overline{M}_1! \overline{M}_2! \overline{M}_{12}!}. \quad (3)$$

Here we have introduced net numbers of occupied sites  $\overline{M}_k = M_k - \overline{M}_{12}$  and of empty sites  $\overline{M}_0 = (L - \overline{M}_1 - \overline{M}_2 - \overline{M}_{12})$ . In the thermodynamic limit the sum of eq. (2) is replaced by its largest term, leading to the relation

$$g^2 = \overline{m}_0 \overline{m}_{12} / (\overline{m}_1 \overline{m}_2) \quad (4)$$

with  $\overline{m}_0 = \overline{M}_0/L$ , etc. Also the expectation values

$$\langle \Psi | \hat{c}_{s\sigma}^+ \hat{c}_{t\sigma} | \Psi \rangle / \langle \Psi | \Psi \rangle = q_\sigma \langle \hat{c}_{s\sigma}^+ \hat{c}_{t\sigma} \rangle_0, \quad s \neq t, \quad (5)$$

are found by combinatorics. Here the ‘‘loss factors’’

$$q_k \equiv \frac{1}{m_k(1 - m_k)} \left[ \sqrt{\overline{m}_k \overline{m}_0} + \sqrt{\overline{m}_{kl} \overline{m}_l} \right]^2 \quad (6)$$

with  $k, l = 1, 2$  and  $k \neq l$  represent the step sizes of the momentum distribution functions at the Fermi level ( $q_k = 1$  for  $g = 1$ ).

When we extend the Gutzwiller method to cases of  $n \geq 2$  correlated orbitals per site, the number of different site occupancies  $J_n = 4^n$  will increase enormously. For  $n = 2$  and using the notation  $a\uparrow \hat{=} 1$ ,  $a\downarrow \hat{=} 2$ ,  $b\uparrow \hat{=} 3$ ,  $b\downarrow \hat{=} 4$  the 16 occupancies are: i) empty ( $\overline{M}_0$ ); ii) four single ( $\overline{M}_k$ ,  $k = 1, \dots, 4$ ); iii) six double ( $\overline{M}_{kl}$ ,  $k, l = 1, \dots, 4; k \neq l$ ); iv) four triple ( $\overline{M}_{klp}$ ) and v) quadruple ( $\overline{M}_{1234}$ ). In general, the  $J_n$  occupancies are labeled by subscripts  $I_j$ , which are assigned to the multiple orbital-spin subscripts by

$$\{I_1, I_2, \dots, I_{2n+1}, I_{2n+2}, \dots, I_{J_n}\} = \{(0), (1), \dots, (2 \cdot n), (12), \dots, (k\dots p)\}. \quad (7)$$

The net and gross occupancies are measured by appropriate operators, e.g.,

$$\widehat{M}_{123} \equiv \sum_s \hat{n}_{s\uparrow}^{(a)} \hat{n}_{s\downarrow}^{(a)} \hat{n}_{s\uparrow}^{(b)} (1 - \hat{n}_{s\downarrow}^{(b)}) = \widehat{M}_{123} - \widehat{M}_{1234}, \quad (8)$$

There are now  $K_n = J_n - (2n + 1)$  multiple occupancies so that the generalized Gutzwiller operator reads as

$$g^{\widehat{D}} \rightarrow \prod_{j=2n+2}^{J_n} (g_{I_j})^{\widehat{M}_{I_j}}. \quad (9)$$

Note, that in contrast to ref. 8, we found it essential to include all multiple occupancies and to use net multiple occupancy operators. The norm is given by

$$\langle \Psi | \Psi \rangle = \prod_{k=1}^n P_k \sum_{\tilde{D}} N_{\tilde{D}} \prod_{j=2n+2}^{J_n} (g_{I_j})^{2\overline{M}_{I_j}} \quad (10)$$

with the  $P_k$  factors of eq. (2), and

$$N_{\tilde{D}} \equiv L! \left[ \prod_{j=1}^{J_n} \overline{M}_{I_j}! \right]^{-1} \quad (11)$$

The sum of eq. (10) includes all sets of multiple occupancy configurations  $\tilde{D} = \{\overline{M}_{I_j}\}$  with  $j = (2n + 2), \dots, J_n$ . Replacing the sum by its largest term leads to the  $K_n$  relations

$$g_{I_j}^2 = \prod_{i=1}^{J_n} (\overline{M}_{I_i})^{\chi_{ij}} \quad , \quad \text{with } \chi_{ij} = \frac{\partial \overline{M}_{I_i}}{\partial \overline{M}_{I_j}} \quad (12)$$

Keeping the gross numbers  $m_k$  fixed, we get

$$\begin{aligned} g_{kl}^2 &= \overline{m}_0 \overline{m}_{kl} / (\overline{m}_k \overline{m}_l) \\ &\dots \\ g_{k..p}^2 &= (\overline{m}_0)^{(\gamma-1)} \overline{m}_{k..p} / (\overline{m}_k \dots \overline{m}_p) \quad , \end{aligned} \quad (13)$$

where  $\gamma$  is the number of subscripts in  $\overline{m}_{k..q}$ . For each of the generalized ‘‘loss factors’’  $q_{kl}$  the evaluation of  $4^{2n-1}$  terms is required. Nevertheless, the resulting equations for the  $q_{kl}$  factors look remarkably simple:

$$q_{kk} = \frac{1}{m_k(1 - m_k)} \left[ \sqrt{\overline{m}_k \overline{m}_0} + \sum_l' \sqrt{\overline{m}_{kl} \overline{m}_l} + \sum_{l,p}'' \sqrt{\overline{m}_{klp} \overline{m}_{lp}} + \sum_{l,p,q}''' \sqrt{\overline{m}_{klpq} \overline{m}_{lpq}} + \dots \right]^2 \quad (14a)$$

$$q_{kl}^2 = q_{kk} q_{ll} \quad (14b)$$

Here the summation primes exclude  $k = l$ , etc. Obviously eqs. (14) are a straightforward generalization of eq. (6) and of results obtained in ref. 4. Simpler forms of the  $q_{kk}$  equations are obtained, when certain multiple occupancies are put zero, as was assumed in ref. 11. Recently, eqs. (14) have also been found by T. Okabe.<sup>12</sup>

Using the generalized Gutzwiller wavefunction, we can now investigate extensions of the Hubbard model for arbitrary numbers of orbitals  $\alpha, \beta$ :

$$\begin{aligned} \widehat{H} = & \sum_{\alpha, \beta, s, t, \sigma} T_{st}^{\alpha\beta} \widehat{\alpha}_{s\sigma}^+ \widehat{\beta}_{t\sigma} + \sum'_{\alpha, \beta, s, \sigma, \sigma'} U^{\alpha\beta} \widehat{n}_{s\sigma}^{\alpha} \widehat{n}_{s\sigma'}^{\beta} \\ & + \sum'_{\alpha, \beta, s, \sigma, \sigma'} J^{\alpha\beta} \widehat{\alpha}_{s\sigma}^+ \widehat{\beta}_{s\sigma'}^+ \widehat{\alpha}_{s\sigma'} \widehat{\beta}_{s\sigma} , \end{aligned} \quad (15)$$

which include, apart from general hopping terms, the on-site interaction  $U$ , both orbital-diagonal ( $U^{\alpha\alpha}$ ) and off-diagonal ( $U^{\alpha\beta}, \alpha \neq \beta$ ), and the on-site or Hund's rule exchange  $J^{\alpha\beta}$ . The primes exclude non-physical orbital-spin combinations in the respective  $U$  and  $J$  summations. For the expectation values of the on-site exchange only the terms

$$- \sum'_{\alpha, \beta, \sigma} J^{\alpha\beta} \widehat{n}_{s\sigma}^{\alpha} \widehat{n}_{s\sigma}^{\beta} \quad (16)$$

survive, i.e., all spin fluctuations are ignored.

By assuming  $J^{\alpha\beta} < U^{\alpha\beta} < U^{\alpha\alpha}$ , it is possible to achieve the filling of incomplete  $d$  shells in the atomic limit according to Hund's rules. Thus, the Hamiltonian of eq. (15) represents realistic models for the valence electron structure of both 3d transition metal elements and of magnetic 3d oxides and halides, provided that a sufficient number of orbitals and sites are included. The  $N$ -particle wavefunctions  $|\Psi\rangle, |\Psi_0\rangle$  can be chosen to represent para-, ferro-, or antiferromagnetic states, and in principle, even more complicated cases, such as orbital ordering. Also, ligand orbitals or  $s, p$  type orbitals on the  $d$  sites may be incorporated. However, any additional complexity of the wavefunctions  $|\Psi_0\rangle$  leads to further variational parameters in  $|\Psi_0\rangle$  representing effective orbital energy shifts or effective hoppings, etc.<sup>4</sup> The problem of orbital density depletion caused by the reduction of multiple occupancies can be treated in analogy to ref. 6.

### III. TWO-BAND MODEL WITH ORBITAL DEGENERACY

In the following, we investigate the  $n = 2$  Hamiltonian, i.e., we assume one atomic site on a simple cubic lattice with two, degenerate  $d(e_g)$  orbitals, and we study only paramagnetic

solutions. The single particle bands are constructed using realistic  $1NN$  and  $2NN$  hopping matrix elements  $T_{dd\sigma}(1NN) = 1eV$ ,  $T_{dd\sigma}(2NN) = 0.25eV$ , and  $T_{dd\delta} : T_{dd\pi} : T_{dd\sigma} = 0.1 : -0.3 : 1$ . There are three interaction parameters  $U^{\alpha\alpha} \equiv U$ ,  $U^{\alpha\beta} \equiv U'$  and  $J^{\alpha\beta} \equiv J$ , which, in the limit of vanishing configuration interaction are related by<sup>13</sup>

$$J = \frac{1}{2}(U - U'). \quad (17)$$

For the paramagnetic case we have  $m_k \equiv m$ ,  $\bar{m}_{klp} \equiv t$ ,  $m_{1234} \equiv f$ ,  $\bar{m}_{12} = \bar{m}_{34} \equiv d_d$ ,  $\bar{m}_{14} = \bar{m}_{23} \equiv d_o$ , and  $\bar{m}_{13} = \bar{m}_{24} \equiv d_t$ . All  $q_{kl}$  are equal

$$q = \frac{1}{m(1-m)} [(\sqrt{d_d} + \sqrt{d_o} + \sqrt{d_t})(\sqrt{\bar{m}} + \sqrt{t}) + \sqrt{\bar{m}_0\bar{m}} + \sqrt{tf}]^2. \quad (18)$$

The energy function for  $e/a \equiv 4m$  (number of electrons per atom) is

$$E = 2q\bar{\epsilon}(m) + 2Ud_d + 2U'd_o + 2(U' - J)d_t + (2U + 4U' - 2J)(2t + f). \quad (19)$$

Here  $2\bar{\epsilon}(m)$  is the kinetic energy of the uncorrelated case.  $E$  has been minimized numerically with respect to the five variational parameters  $d_d, d_o, d_t, t, f$  and has been studied at several  $m$  values and for various sets of interaction parameters  $U$  and  $u' \equiv U'/U$ , keeping  $2J = U - U'$  according to eq. (17).

There are two  $m$  regions of interest. The first is around  $m = 0.25$  (or  $m = 0.75$ ), the other around  $m = 0.5$ . For these integer fillings ( $e/a = 1, 2, 3$ ) we observe metal-insulator (MI) transitions in the  $(U, u')$ -plane. However, there are big differences between the two cases, mainly concerning the shapes of the phase diagrams in the  $(U, u')$ -plane and the order of the MI transitions.

For  $m = 0.25$ , the MI phase diagram is shown in Fig. 1a. For  $u' = 1$ , we find  $U_C \approx 13.8$  in agreement with ref. 11. For  $u' > 1/3$  ( $U' > J$ ) the system will avoid all multiple occupancies in the limit  $U \rightarrow \infty$ , so that there is always a MI transition. This transition is of second order in  $q$ , very similar to that of the one-band model.<sup>9</sup> Near any critical values  $(U_C, u'_C)$ ,

$q$  behaves like  $q \approx q_0(1 - U/U_C)$ , when we approach  $U_C$  from the metallic side, i.e.; the effective mass  $m^* = m_e/q$  diverges with  $(1 - U/U_C)^{-1}$ .<sup>9,10</sup> For  $u' \leq 1/3$  ( $U' \leq J$ ) the system is always metallic.

In contrast, the MI transition for  $m = 0.5$  is very different (see Fig. 1a). The transition is generally of first order in  $q$ . This means that the  $q$  values change discontinuously at critical values  $(U_C, u'_C)$  from a metal (typically  $q \approx 0.6$ ) to an insulator ( $q = 0$ ) (see Fig. 1b). Only at the point  $u' = 1$  (i.e.  $U_C = U'_C$ ) the MI transition is second order in  $q$ . Note that apart from the point  $u' = 1$  the ground state energy  $E$  varies at the transition in such a way that its first derivatives with respect to all relevant system parameters changes discontinuously. In particular we observe a finite discontinuity of the chemical potential  $\mu(m) = \partial E(m)/\partial m$  at  $m = 0.5$  for all  $u' < 1$  if  $U$  exceed  $U_C$  by any infinitesimal amount.

In the insulating region we have  $t = f = 0$ , and because of particle hole symmetry,  $\bar{m}_0 = \bar{m} = 0$ . For  $u' < 1$  only the spin triplet occupancy  $d_t$  prevails:  $d_t = 0.5$ ,  $d_d = d_o = 0$ . The case  $u' = 1$  is special, as there is no preference for one of the three double occupancies. We believe, because of this kind of frustration the metallic phase extends so far out near  $u' \lesssim 1$ .

In the metallic regime all multiple occupancies are nonzero (see Fig. 2). For  $u' < 1$ ,  $d_t$  increases with  $U$ , typically up to  $d_t \approx 0.25$ . Then, at  $U_C$ ,  $d_t$  jumps up to 0.5, representing a low-to-high-spin transition. For certain band filling values close to  $m = 0.5$ , the first order step is still present in the  $q(U, u')$  and  $d_t(U, u')$  curves. Further away from  $m = 0.5$ , the curves smoothen, yet still vary rapidly in the range of critical parameters  $(U_C, u'_C)$  as shown in Fig. 2. A typical phase diagram in the  $(U, u')$ -plane of this “good-to-bad”-metal or low-to-high-spin transition is shown in Fig. 3.

Note that for our evaluation a homogenous phase was assumed. However, in the vicinity of the low-to-high-spin transition, the homogeneous phase is unstable against phase separation. As a consequence there exists a surface  $m_{ps}(U, u')$  in the space of  $(U, u', m)$  which divides the homogeneous from the separated region (see Fig. 3). At any point  $(U, u', m)$

with  $m_{ps} < m < 0.5$  (or  $m'_{ps} > m > 0.5$ ), the system breaks up into one part with density  $m_1 = 0.5$  and another one with  $m_2 = m_{ps}(m'_{ps})$ . It is an open question, however, whether the phase separation is an artefact of Hubbard-type models, because of, e.g., the neglect of long range Coulomb interaction.

The first order behavior of the MI transition for  $m = 0.5$  is caused by the competition of two different energy minima, now possible due to of the much larger space of variational parameters. We expect that the first order nature will survive when we include antiferromagnetic states in the minimization. First order, low-to-high spin transitions are also observed for two-band, itinerant ferromagnetic states.<sup>14</sup> In fact, we suspect that first order changes in the electronic structure of incomplete 3d shells may drive many phase transitions of magnetic 3d compounds. It should be interesting to reexamine the MI phase transitions observed e.g. for  $NiS$ ,  $NiJ_2$  or  $RENiO_3$ <sup>15-17</sup> with respect to their first order behavior.

Very recently, a dynamical mean field study about the MI transition in a degenerate ( $n=2$ ) Hubbard model has been presented.<sup>18</sup> The authors only consider the cases  $J = 0$  and/or  $m \leq 0.25$  (in our notation). In agreement with our results, they find a qualitative feature, which is very similar to the  $n = 1$  case. Nevertheless, their more general remark that the nature of the Mott transition is not qualitatively changed by orbital degeneracy is not supported by our results, concerning the cases  $J > 0$ ,  $m \approx 0.5$ .

#### IV. CONCLUDING REMARKS

In conclusion, we have extended the Gutzwiller method to arbitrary numbers  $n \geq 2$  of correlated orbitals per site and have reported studies on the simplest  $n = 2$  model. We find a wealth of new features, not present in the  $n = 1$  models, such as first order metal-insulator transitions or low-to-high spin transitions. Numerical studies appear to be feasible even for  $n = 5$  realistic models of 3d transition metals and compounds.

Acknowledgments: This work has been partly supported by the European Union Human Capital and Mobility program, Project No. CHRX-CT 93-0332



## REFERENCES

- <sup>1</sup> M. C. Gutzwiller, Phys. Rev. Lett. 10, 159 (1963); M. C. Gutzwiller, Phys. Rev. 137, A1726 (1965)
- <sup>2</sup> T. Ogawa, K. Kanda, and T. Matsubara, Prog. Theor. Phys. 53, 614 (1975); F. Takano and M. Uchinami, Prog. Theor. Phys. 53, 1267 (1975); J. Florencio and K. A. Chao, Phys. Rev. B14, 3121 (1976)
- <sup>3</sup> W. Metzner, Z. Phys. - Condensed Matter 77, 253 (1989); P. Fazekas, B. Menge, and E. Müller-Hartmann, Z. Phys. - Condensed Matter 78, 69 (1990)
- <sup>4</sup> C. M. Varma, W. Weber, and L. J. Randall, Phys. Rev. B33, 1015 (1985)
- <sup>5</sup> T. M. Rice and K. Ueda, Phys. Rev. B34, 6420 (1986)
- <sup>6</sup> V. Z. Vulovic and E. Abrahams, Phys. Rev. B36, 2614 (1987)
- <sup>7</sup> W. Metzner and D. Vollhardt, Phys. Rev. B37, 7382 (1988)
- <sup>8</sup> K. A. Chao and M. C. Gutzwiller, J. Appl. Phys. 42, 1420 (1971); K. A. Chao, Phys. Rev. B4, 4034 (1971); Phys. Rev. B8, 1088 (1973)
- <sup>9</sup> W. F. Brinkmann and T. M. Rice, Phys. Rev. B2, 4302 (1970)
- <sup>10</sup> D. Vollhardt, Rev. Mod. Phys. 56, 99 (1984)
- <sup>11</sup> J. P. Lu, Phys. Rev. B49, 5687 (1994), and preprint
- <sup>12</sup> T. Okabe, J. Phys. Soc. Jpn. 65, 1056 (1996)
- <sup>13</sup> S. Sugano, Y. Tanabe and H. Kamimura, "Multiplets of Transition-Metal Ions in Crystals" in Pure and Applied Physics, Vol 33
- <sup>14</sup> J. Bünemann and W. Weber, to be published
- <sup>15</sup> M. P. Pasternak, R. D. Taylor, A. Chen, C. Meade, L. M. Falicov, A. Gieseckus, R. Jeanloz, and P. Y. Yu, Phys. Rev. Lett. 65, 790 (1990);

- <sup>16</sup> J. T. Sparks and T. Komoto, Phys. Lett. 25A, 398 (1967); A. Fujimori, K. Terakura, S. Ogawa, M. Taniguchi, S. Suga, M. Matoba, and S. Anzai, Phys. Rev. B 37, 3109 (1988);
- <sup>17</sup> J. B. Torrance, P. Lacorre, A. I. Nazzal, E. J. Ansaldo, and Ch. Niedermayer, Phys. Rev. B, 45, 8209 (1992)
- <sup>18</sup> H. Kajueter and G. Kotliar, preprint (Sissa server cond-mat/9609176)

## FIGURES

FIG. 1. a) Phase diagrams in the  $(U, u')$ -plane of metallic and insulating phases for  $m = 0.25$  (dashed line, LH scale  $U_1$ ) and for  $m = 0.5$  (solid line, RH scale  $U_2$ ). The lines separate the metallic phases (small  $U$ ) from the insulating phases (large  $U$ ). For  $m = 0.5$  the insulating phase is a triplet state ( $d_t = 0.5$ ) for  $u' < 1$ , and a singlet state ( $d_d = 0.5$ ) for  $u' > 1$ . b) Loss factor  $q_C$  at the MI transition points  $(U_C, u'_C)$ .

FIG. 2. Double ( $d_t, d_d, d_o$ ), triple ( $t$ ) and quadruple ( $f$ ) occupancies for  $m = 0.5$  ( $e/a = 2$ ) as a function of  $U$ , with  $u' = 0.8$  (solid lines). Also shown are  $d_t(U)$  curves for  $m = 0.49, 0.48, 0.47$ , respectively, indicating the “good-to-bad” metal transition away from  $m = 0.5$ .

FIG. 3. Phase diagrams in the  $(U, m)$ -plane, with  $u' = 0.8$ : Lines dividing the “good metal” from the “bad metal” phases are indicated by  $m_{gb}$ , lines dividing the homogeneous from the phase separated regions are denoted by  $m_{ps}$ . For the part of  $m_{gb}$  given by dashed lines, the discontinuity in  $q(U, u')$  has disappeared; here inflection points are used to determine the phase boundary.

Figure 1

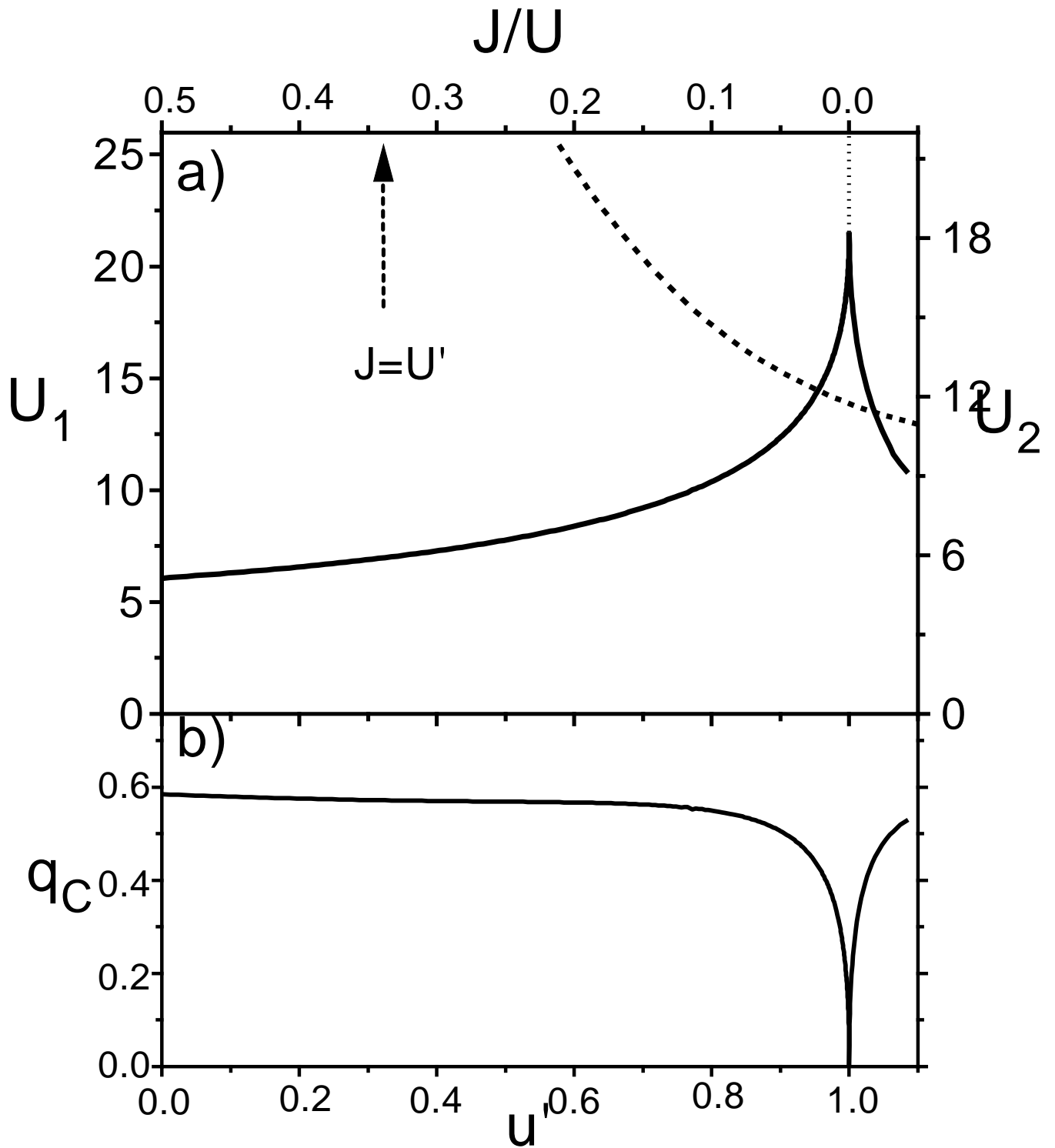


Figure 2

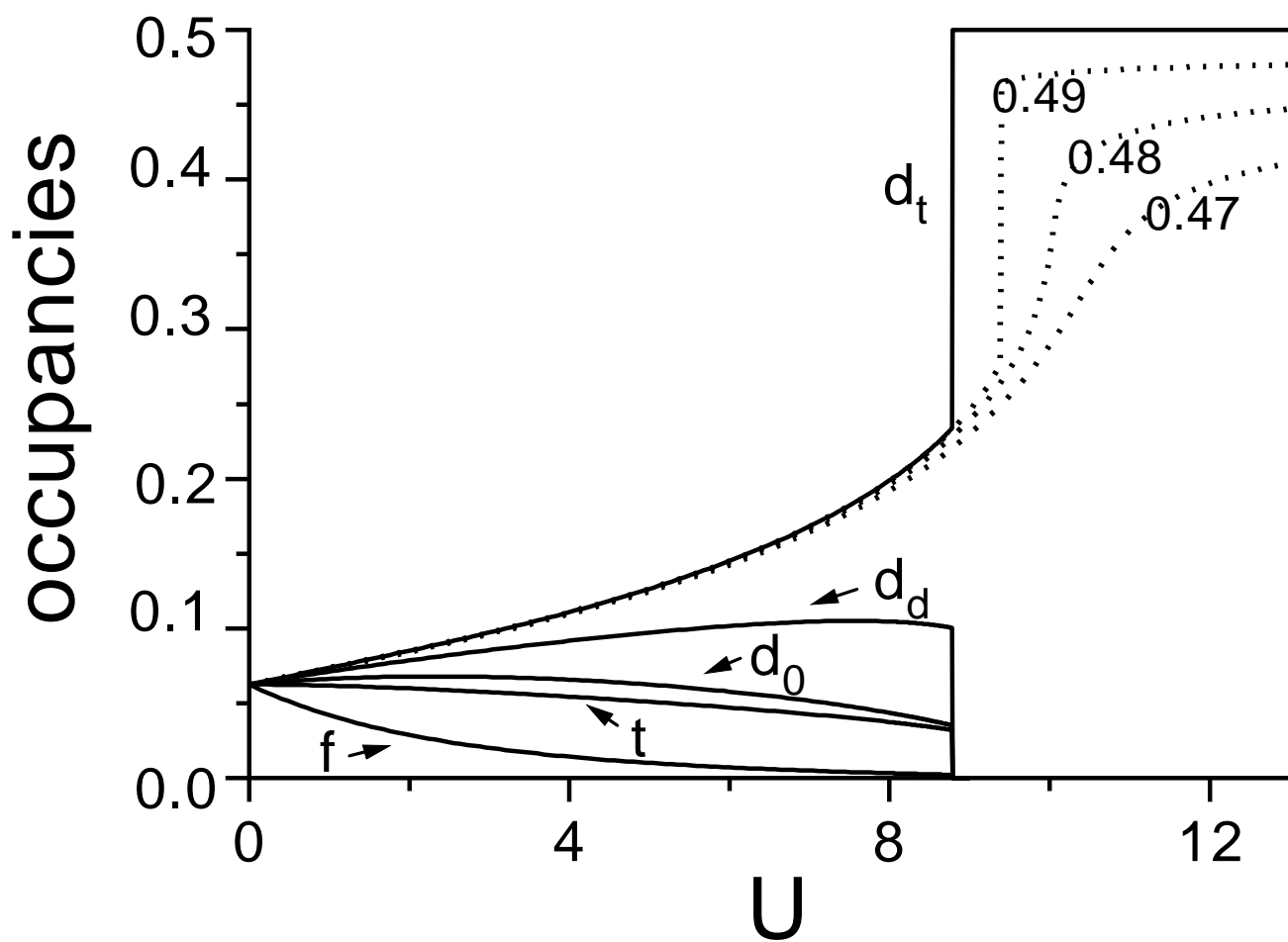


Figure 3

